

Size-dependent surface energies of Au nanoparticles

D. Holec,^{1,*} P. Dumitraschkewitz,¹ F.D. Fischer,² and D. Vollath³

¹*Department of Physical Metallurgy and Materials Testing,
Montanuniversität Leoben, Franz Josef Straße 18, A-8700 Leoben, Austria*

²*Institute of Mechanics, Montanuniversität Leoben, Franz Josef Straße 18, A-8700 Leoben, Austria*

³*Nano Consulting, Primelweg 3, D-76297 Stutensee, Germany*

(Dated: November 1, 2018)

Motivated by often contradictory literature reports on size dependence of surface energy of gold nanoparticles, we performed an atomistic study combining molecular dynamics and *ab initio* calculations. We show that in the case of nanocubes, their surface energy converges to a value for (001) facets of bulk crystals. A fast convergence to a single valued surface energy is predicted also for nanosheres. Here, however, the value is larger than the surface energy of any low-index surface facet of bulk Au crystal. This is explained by the complex structure of the surface with an extensive number of broken bonds due to edge and corner atoms. A similar trend was obtained also for the case of cuboctahedron-shaped nanoobjects. As the exact surface area of the nanoparticles is an ill-defined quantity, we introduced the surface-induced excess energy and discussed this quantity as a function of (i) number of atoms forming the nanoobject or (ii) its characteristic size. In the former case, a universal power-law behaviour was obtained independent of the nanoparticle shape.

PACS numbers: 31.15.A-, 61.46.Df, 68.35.Md, 83.10.Rs

I. INTRODUCTION

Whenever one discusses thermodynamics or any other feature of nanoparticles, surface energy is one of the key properties. **This is due to the fact that volume-to-surface ratio is fast decreasing with decreasing nanoparticle size, hence enhancing influence of the surface properties. For example, it has been repeatedly reported that modification of the surface energy leads to the change of the nanoparticle shape^{1,2}.** It is, therefore, surprising that **for many materials** this is a rather poorly known material property, especially when it comes to small particles with characteristic dimension less than 5 nm. In many cases one finds decreasing surface energy with decreasing particle size, e.g., in a study by Vollath and Fischer³ or earlier studies^{4,5}. This trend is conventionally explained with an increasing tendency to form a liquid-like structure at the surface of the particles⁶. On the other hand, there exists a series of primarily theoretical papers finding a significant increase of the surface energy with decreasing particle size, see, e.g., Refs. 7 or 8. Furthermore, there are also some heavily disputed experimental results pointing in the direction of increasing surface energy with decreasing particle size^{9,10}. **Nanda *et al.*¹⁰ pointed out, that the difference between various reported trends stems from the nanoparticle nature: for free nanoparticles, the surface energy is expected to increase with decreasing particle size, while the opposite trends is obtained for nanoparticles embedded in a matrix.**

Despite similar studies have been performed for other systems, e.g. Ag^{7,8}, we are not aware of a theoretical report concerning specifically gold nanoparticles. Moreover, the previous reports did not discuss the effect of nanoparticle shape. It is the purpose of this study to shed some light on this dissenting situation by theoretical methods of atomistic modelling. To unveil basic princi-

ples we consider **free** nanoparticles with idealised shapes carved out of infinitely large bulk material, and subsequently structurally relaxed. This study addresses surface energy of gold nanoparticles, i.e., interfaces between gold nanoparticle with well defined shape, and vacuum. We note that this makes our results different from experiments in which a solid-liquid interface is of crucial importance during the forming process, in addition to irregular shapes obtained in experimental reality.

II. METHODOLOGY

Molecular dynamics (MD) simulations were performed using the LAMMPS package¹¹ together with an **interatomic potential** describing the gold-gold interaction within the embedded atom method (EAM) as parametrised by Grochola *et al.*¹². The individual idealised nanoparticles with well-defined shapes were cut out from bulk fcc structure with lattice constants of 4.0694 Å. This was obtained from fitting calculated total energies corresponding to different bulk volumes with Birch-Murnaghan equation of state¹³, and agrees well with the values 4.0701 Å obtained by Grochola *et al.*¹². All structural models were relaxed using conjugate-gradient energy minimisation scheme with force-stopping convergence criterion set to 10⁻¹² eV/Å. **The rectangular simulation box was ≈ 10 Å larger than the nanoparticles in order not to limit the relaxation procedure.**

Additionally, a few *ab initio* runs were performed to benchmark our MD calculations. We used Vienna Ab initio Simulation Package (VASP)^{14,15} implementation of Density Functional Theory (DFT)^{16,17}. The plane wave cut-off energy was set to 400 eV, and the reciprocal space sampling was equivalent to 10 \times 10 \times 10 *k*-mesh for the fcc-conventional cell. Two common approxima-

tions of the electronic exchange and correlation effects were considered: local density approximation (LDA)¹⁷ and the Perdew-Wang parametrisation of the generalised gradient approximation (GGA)¹⁸. The contribution of ions and core electrons were described by projector augmented wave (PAW) pseudopotentials¹⁹. **Due to the employed periodic boundary conditions, we used simulation box ≈ 20 Å larger than the actual (unrelaxed) nanoparticle to avoid any undesired interactions through the vacuum separating neighbouring nanoparticles. Similarly, ≈ 15 Å vacuum in the direction perpendicular to a free surface was used to separate slabs for calculating the surface energies of bulk Au (both for MD and DFT calculations).**

III. RESULTS AND DISCUSSION

A. Low-index facets of bulk Au

The results presented in this chapter serve the subsequent discussion of the MD results, and their accuracy with respect to first principles calculations. Surface energy γ of surface facet (hkl) can be calculated as

$$\gamma = \frac{1}{2A} (E_{\text{slab}} - NE_{\text{bulk}}) , \quad (1)$$

where E_{slab} is energy of a slab composed of N layers. E_{bulk} is the energy of the bulk material per one layer of cross-section A . The factor 2 result from the fact that the slab has two surfaces. A layer is understood as a surface primitive cell, i.e. when the desired facet (hkl) is perpendicular to one of the lattice vectors (for a detailed description of the surface primitive cells, see e.g., Ref. 20). Due to the interaction of the two free surfaces through either vacuum (i.e., not well separated slabs in the case of periodic boundary conditions) or the bulk of the slab (i.e., too thin slab) the value γ has to be converged with respect to both of these. In the case of MD simulations, only the latter convergence needs to be tested when the simulation is run in a box without periodic boundary conditions in the direction perpendicular to the free surface.

An example of such a convergence behaviour is shown in Fig. 1. From here it becomes clear that 10 Å vacuum is enough while at least $N = 10$ (21 atoms) layers were needed to get a constant value of γ for (100) surface of gold. Similarly, at least $N = 12$ (25 atoms) layers were needed for the (110) surface, while $N = 6$ layers (19 atoms) was enough for the case of (111) surface.

The obtained values from the DFT benchmarks and MD simulations are summarised in Table I. The here obtained DFT values are comparable with data from the literature. They exhibit the same ordering ($\gamma_{(110)} > \gamma_{(100)} > \gamma_{(111)}$) as reported in earlier²¹. In a simplified picture, the surface energy expresses energy penalty related to the areal density of broken bonds^{20,22}. This is $8/a_0^2$ for the (100) surface, $7.07/a_0^2$ for (110), and

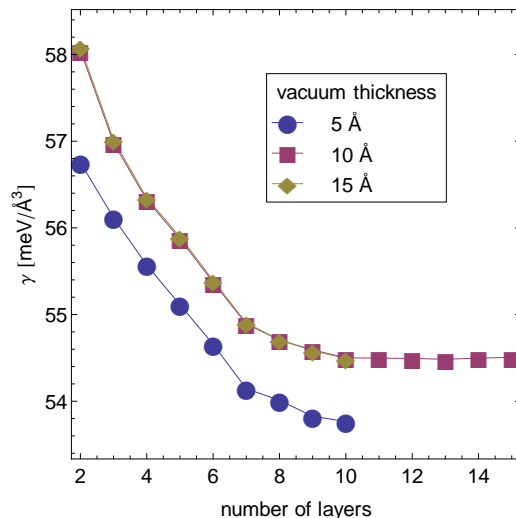


FIG. 1: GGA-DFT values of γ calculated from Eq. 1 for (100) surface of Au.

$4.33/a_0^2$ for the (111) surface (a_0 being the fcc lattice constant). The density of broken bonds is similar for the (100) and (110) surfaces, while it is significantly lower for the (111) orientated facet, hence providing a rough explanation for the surface energy ordering.

The DFT and MD values have almost a constant difference between corresponding surface energies. Moreover, the MD values are very close to the DFT-LDA results. This maybe somewhat surprising since the EAM potential has been fitted to the GGA-DFT data using the same parametrisation by Perdew and Wang¹⁸. We speculate that this is caused by fixing 4.07 Å as the lattice constant during the EAM potential fitting¹², as our LDA and GGA calculations yielded 4.061 and 4.176 Å, respectively. Nevertheless, since LDA and GGA are known to overestimate and underestimate, respectively, binding²³, and since the MD values are in between the two DFT-based estimations, we conclude that the interatomic potential used here is suitable for studying trends in surface energies. Moreover, the resulting values are expected to be very close to DFT-LDA calculations.

B. Impact of shape and size on the nanoparticles surface energy

1. Nanocubes

{100}-faceted nanocubes with a side length up to 20 nm were structurally relaxed. As a consequence of the surface tension, the apexes “popped in” as it is apparent from the snapshots before and after optimisation overlaid in Fig. 2.

When using DFT, it was feasible to handle nanocubes only up to the $3 \times 3 \times 3$ size (172 atoms), while nanocubes up to $50 \times 50 \times 50$ (515 151 atoms) were calculated using

	(100)		(110)		(111)	
	[meV/Å ²]	[J/m ²]	[meV/Å ²]	[J/m ²]	[meV/Å ²]	[J/m ²]
GGA-DFT (this work)	54.5	0.87	57.0	0.91	45.2	0.72
GGA-DFT (Ref. 24)					50	0.80
GGA-FCD (Ref. 21)	101.5	1.63	106.1	1.70	80	1.28
MD (this work)	80.9	1.30			72.5	1.16
LDA-DFT (this work)	83.5	1.34	89.2	1.43	78.4	1.26
LDA-DFT (Ref. 24)					80	1.28
experiment (Ref. 25)					93.6	1.50
experiment (Ref. 26)					94.0	1.51

TABLE I: Surface energies, collection also from literature. FCD = full charge density

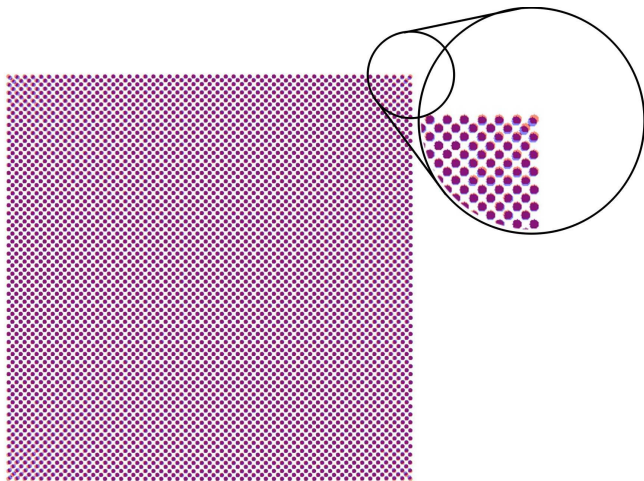


FIG. 2: Overlaid snapshots of starting (ideal, red) and final (relaxed, blue) configuration for nanocube with side $a = 20.3$ nm (515 151 atoms).

MD. The surface energy was evaluated as

$$\gamma = \frac{E_{\text{nanocube}} - NE_{\text{bulk}}}{6 \times A}, \quad (2)$$

where E_{nanocube} is the energy of a nanocube formed from $n \times n \times n$ cubic conventional fcc cells (4 atoms per cell), $N = 4n^3 + 6n^2 + 3n + 1$ is the number of atoms in the nanocube, E_{bulk} is the energy per atom of bulk Au, and $A = a_0 n^2$ is the surface area (a_0 is the bulk lattice constant, i.e., the surface energy is evaluated with respect to the unrelaxed surface area, i.e., the reference configuration). The calculated values shown in Fig. 3 were fitted with an exponential relationship

$$\gamma = \gamma_0 \exp\left(\frac{\mathcal{A}}{a}\right), \quad (3)$$

where a is the side length of the cube. The thus obtained values of the pre-exponential parameter, $\gamma_0^{\text{GGA}} = 53 \text{ meV}/\text{\AA}^2$, $\gamma_0^{\text{LDA}} = 83 \text{ meV}/\text{\AA}^2$, and $\gamma_0^{\text{MD}} = 80 \text{ meV}/\text{\AA}^2$ agree well with the bulk surface energies for the (100) facets ($\gamma_{(100)}^{\text{GGA}} = 54.5 \text{ meV}/\text{\AA}^2$, $\gamma_{(100)}^{\text{LDA}} = 83.5 \text{ meV}/\text{\AA}^2$,

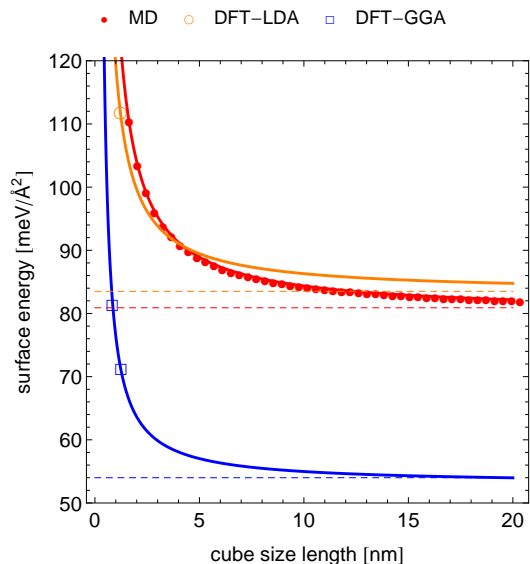


FIG. 3: Surface energy of nanocubes. The calculated datapoints were fitted with Eq. 3. The dashed lines are (100) surface energies as listed in Table I.

and $\gamma_{(100)}^{\text{MD}} = 80.9 \text{ meV}/\text{\AA}^2$). This is an expected result as the bulk values are limits for infinitely large cubes. It is, however, surprising, that such a good agreement is obtained for the DFT data where only three data points are available for the fitting procedure. The same fitting procedure yielded for the parameter \mathcal{A} (Eq. 3) values of 0.365 nm, 0.360 nm, and 0.524 nm for DFT-GGA, DFT-LDA, and MD data sets, respectively.

2. Nanospheres

As an opposite extreme to the nanocubes with single orientated sides, nanospheres with varying radii were considered. These were constructed by cutting material contained in an ideal sphere of a given radius out of the infinitely large fcc cell of Au. The DFT calculations were performed up to $r = 0.9$ nm (152 atoms), while the MD calculations run for spheres up to $r = 20.3$ nm

(2094177 atoms), see Fig. 4a. The exact surface area of a nanosphere is ill-defined especially for small nanoparticles. (Questions may be asked as: What is the radius? And is the surface a sphere, or should it follow atomic steps?) We therefore use the cut-off radius, R , of unrelaxed nanoparticle to define an approximate spherical surface for evaluation of the surface energy as

$$\gamma = \frac{E_{\text{nanosphere}} - NE_{\text{bulk}}}{4\pi R^2}. \quad (4)$$

Unlike in the case of nanocubes, the MD surface energy of the nanospheres converges relatively quickly to a constant value of $\approx 94 \text{ meV}/\text{\AA}^2$. This is a slightly higher value than γ of any low-index facet (cnf. Table I) reflecting the fact that a spherical surface composes (from the atomistic point of view) of a large number differently orientated facets. Places where these facets meet (i.e. edges) are composed of atoms with the same or higher number of broken bonds than atoms in the surrounding planar facets, thus further increasing the surface energy.

The surface energies were evaluated with respect to the unrelaxed surface area to make it comparable with other shapes where the estimation of surface area of relaxed structures is non-trivial. The spherical shape, however, allows to estimate the influence of the structural relaxation near to the surface. For every relaxed nanosphere a minimum radius of a sphere containing all atoms was established, and the surface energy was re-evaluated with this new value which was smaller than the original unrelaxed radius. Consequently, the surface energy increases as shown in Fig. 4b. The error caused by neglecting the surface relaxation becomes negligible for sphere radii $\gtrsim 5 \text{ nm}$. The largest discrepancies between the relaxed and unrelaxed geometry estimations are for nanospheres with radii $\lesssim 3 \text{ nm}$. However, due to the extremely small object sizes the atomistic nature cannot be neglected here, and thus the whole analysis using a spherical surface is questionable for “spheres” composed of only several hundreds of atoms.

3. Cuboctahedrons

The last class of objects studied in this work are cuboctahedrons, i.e., (100)-faceted cubes with all apexes cut by (111) planes (see inset in Fig. 5). The surface energy shown in Fig. 5 was evaluated with respect to the unrelaxed surface area:

$$\gamma = \frac{E_{\text{nanosphere}} - NE_{\text{bulk}}}{(3 + \sqrt{3})a^2}, \quad (5)$$

where a is the length of the edge of the cube from which the cuboctahedron is formed.

It can be seen that the surface energy oscillates between two values, ≈ 78 and $\approx 90 \text{ meV}/\text{\AA}^2$. This behaviour is caused by the changing ratio of surface atoms forming the (100) and (111) facets and the edges and

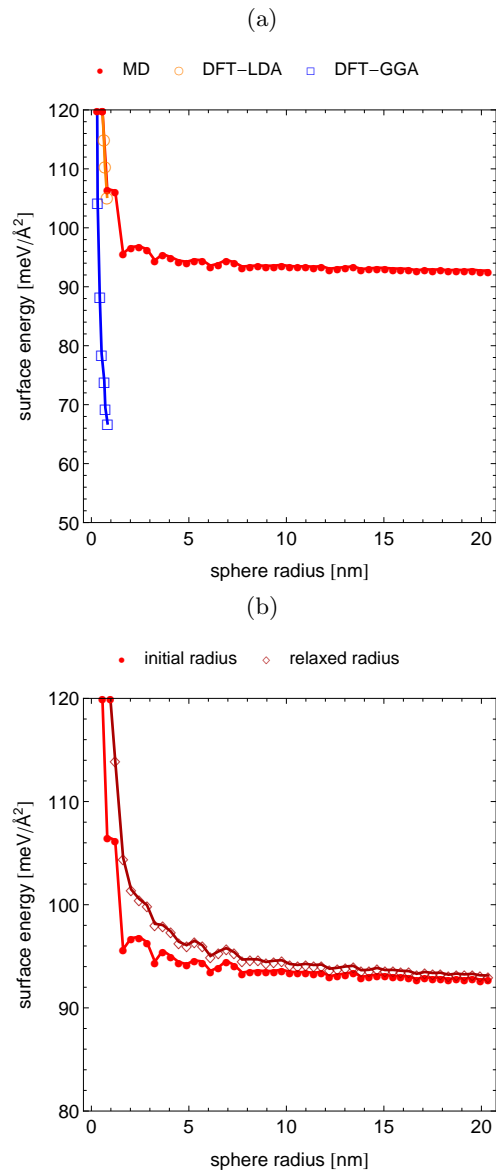


FIG. 4: (a) Surface energy of nanospheres calculated by DFT and MD. (b) Comparison of surface energy evaluated with respect to unrelaxed and relaxed surface area.

corners, which directly corresponds with the atomistic nature of the nanoobjects. A detailed analysis of the coordination of the surface atoms reveals that the number of 9-coordinated surface atoms corresponding to ideal (111) facets, is in anti-phase with the surface energy as shown in Fig. 5. The 8-coordinated (100) surface atoms also show small steps hence causing a non-monotonous increase of their number as a function of the cuboctahedron size. At the same time, number of 10-, 7-, 6-, and 5-coordinated surface atoms, corresponding to edges and corners (i.e., atoms with even smaller coordination and, consequently, more broken bonds than those on ideal (100) and (111) facets), and hence increasing the overall

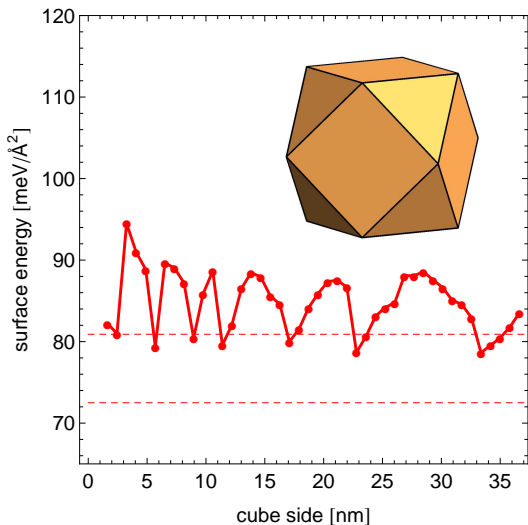


FIG. 5: Surface energy of cuboctahedrons as a function of the size of “parent” cube.

surface energy, exhibits the same “oscillations” with the cuboctahedron size as the surface energy itself. As such, the oscillations are expected to decrease with increasing cuboctahedron size. It is interesting to note that the two limit values for the surface energies represent the same range as the two values, 80.9 and 72.5 meV/Å² for pure (100) and (111) facets, respectively. Similarly to the case of nanospheres, the values are somewhat higher than the ideal single-orientated facets due to the presence of the edges.

C. Surface induced excess energy

In order to eliminate the above described problem with estimation of the exact surface area of the nanoobjects, we introduced a new quantity expressing the surface-induced excess energy with respect to the bulk energy corresponding to the same amount, N , of atoms which compose the nanoobject:

$$E_{\text{excess}} = \frac{E_{\text{object}} - NE_{\text{fcc-Au}}}{N}, \quad (6)$$

where $E_{\text{fcc-Au}}$ is the energy per atom of ideal bulk fcc-Au. A similar concept has been previously demonstrated to work also for energetics of carbon fullerenes²⁷, or even for elasticity of nanoporous gold²⁸. If the excess energy is evaluated for nanocubes, nanospheres, and cuboctahedrons, a linear relationship between $\log E_{\text{excess}}$ and $\log N$ is obtained independent of the nanoparticle shape (Fig. 6a). This suggests that the excess energy is a power law function of the total number of atoms (object size).

This fit (the solid line in Fig. 6a) gives

$$E_{\text{excess}} = 3523.3 \text{ meV/atom} \times N^{-0.346}. \quad (7)$$

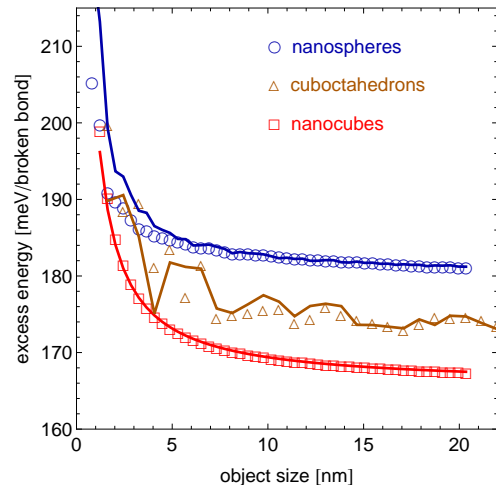
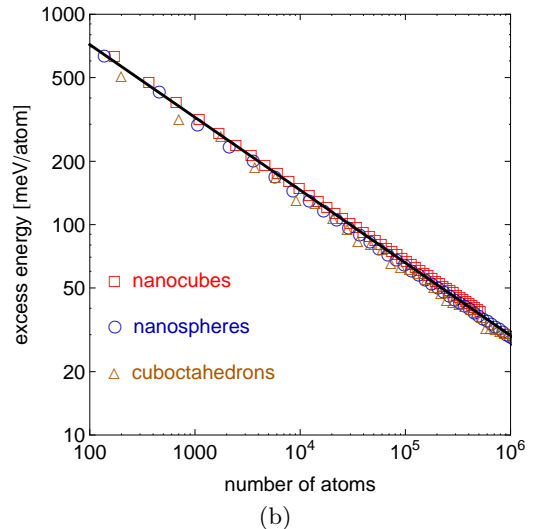


FIG. 6: Excess energy of nanoobjects with respect to the bulk Au (a) as a function of the number of atoms forming the nanoobject, and (b) divided by the number of broken bonds and expressed as a function of the nanoobject size.

Recalling the idea that the surface energy is genuinely connected with the broken bonds (bb), we now establish the energy needed to “break” a bond. An $n \times n \times n$ nanocube contains atoms with 4 different nearest neighbour coordinations: 8 atoms with 9 bb forming corners (i.e., 3-coordinated atoms), $(12n - 12)$ atoms with 7 bb forming the edges (i.e., 5-coordinated atoms), $(12n^2 - 12n + 6)$ atoms with 4 bb forming the surface facets (i.e., 8-coordinated atoms), and $(4n^3 - 6n^2 + 3n - 1)$ bulk atoms with no bb (i.e., fully 12-coordinated atoms). If we simply assume that all bonds “cost” the the same energy E_{bond} to break them, and express the excess energy as

$$E_{\text{excess}} = [9 \times 8 + 7 \times (12n - 12) + 4 \times (12n^2 - 12n + 6)] E_{\text{bond}} , \quad (8)$$

we obtain $E_{\text{bond}} = 167.9$ meV/bond from fitting the data for nanocube sizes up to 20 nm.

However, the red squares in Fig. 6b clearly exhibit a non-constant value for E_{bond} . Consequently, we propose a slightly modified description in which the energy needed to break a bond is a function of the coordination. Hence, it costs different energy to create, e.g., a corner atom (9 broken bonds) than a facet atom (4 broken bonds). The excess energy was, therefore, fitted with

$$E_{\text{excess}} = 72E_{\text{corner}} + 84(n-1)E_{\text{edge}} + 24(2n^2 - 2n + 1)E_{\text{facet}} \quad (9)$$

yielding $E_{\text{corner}} = 277.8$ meV/bond, $E_{\text{edge}} = 217.9$ meV/bond, and $E_{\text{facet}} = 165.7$ meV/bond. The fitted values of the excess energy, normalised to the number of bonds, are plotted in Fig. 6b with the red solid line. It turns out that for nanocubes with side $\gtrsim 5$ nm, Eq. 9 provides predictions with an accuracy better than ≈ 1 meV/bond. Energy of a broken bond corresponding to an infinitely large (100) facet can be estimated from the surface energies as given in Table I. This value is 167.5 meV/bond, which is close to E_{bond} (Eq. 8) as well as E_{facet} (Eq. 9).

The complex shapes of cuboctahedrons and nanospheres somewhat restrict the intuitive analysis of the excess energy above presented. When the excess energy is fitted with a single valued energy per broken bond (equivalent to Eq. 8), values of 172.4 and 181.6 meV/bond are obtained for cuboctahedrons and nanospheres, respectively. These values represent an excellent estimation of the excess energies in the limit of large nanoparticles, as shown in Fig. 6b. Moreover, the value for cuboctahedrons lies between the values estimated for (100) ($E_{(100)} = 167.5$ meV/bond) and (111) ($E_{(111)} = 173.3$ meV/bond) facets. This further illustrates that the surface energy values as presented in Sec. III B are hugely influenced by the evaluation of the actual surface area (which is, from the atomistic point of view, ill-defined). Consequently, the mean value of the surface energy of cuboctahedrons as shown in Fig. 5 lies outside the range defined by $\gamma_{(100)}$ and $\gamma_{(111)}$.

Finally, in order to obtain a non-constant behaviour, we fit the excess energy with

$$E_{\text{excess}} = \sum_{i=1}^{11} (12 - i)N(i)E(i) \quad (10)$$

where $N(i)$ is the number of i -coordinated atoms (i.e. those having $(12 - i)$ broken bonds) and $E(i)$ is the corresponding excess energy contribution. Eq. 10 is a generalised formulation of Eq. 9 reflecting that all possible coordinations may occur due to the shape of nanoparticles. We note that the smallest coordination obtained was 3 and 4 for the case of cuboctahedrons and nanospheres,

respectively. The fitted values of $E(i)$ are given in Table II, and the corresponding excess energies are shown in Fig. 6b with solid lines. In particular, the fit provides an excellent agreement with the MD predicted surface excess energies for nanospheres.

Our analysis provides an insight into the trend predicted here. Regardless of the nanoparticle shape, the surface energy decreases with the increasing particle size. The reason is that the smaller the nanoparticle the larger is the fraction of surface atoms with small coordination, i.e. those with lots of broken bonds. Moreover, the energy to break a bond increases with the decreasing atom coordination.

D. Contribution of surface stress state

As it has been recently stressed out²⁹, the excess energy due to a free surface has two contributions: surface energy related to the energy penalty of broken bonds, and elastic strain energy due to the surface stress state. The latter is generated by a surface curvature, which maintains the mechanical force equilibrium between the surface stress state and the body stress state. As an illustrative example let us assume a spherical body and a homogeneous surface stress state with the value σ acting on it, which leads to a pressure with value $2\sigma/R$ in the whole spherical body. From this description it becomes clear that the surface stress contribution is zero for the slab approach to calculate surface energy as presented in the section III A. Similarly, the surface stress contribution will be negligible for larger nanocubes with only a marginal fraction of corner and edge atoms (see discussion in the section III C).

We now try to estimate the surface stress contribution to the excess energy for the case of a spherical nanoparticle using classical continuum mechanics. Let's denote R the nanosphere's radius, and γ its surface energy. Furthermore, let's keep to the reasonable assumption that the value of σ and γ are of the same order of magnitude. The corresponding total surface energy is then

$$\mathcal{E}_\gamma = 4\pi R^2 \gamma . \quad (11)$$

For the sake of simplicity we further assume isotropic elastic properties of the nanoparticle, with ν and E being its Poisson's ratio and Young's modulus, respectively. The strain energy caused by the surface stress σ , causing internal pressure $2\sigma/R$, is

$$\mathcal{E}_\sigma = \frac{4}{3}\pi R^3 \frac{6(1 - 2\nu)}{E} \frac{\sigma^2}{R^2} , \quad (12)$$

for details see, e.g. Ref. 30, Appendix 3. The ratio of the surface stress strain energy to surface energy then is

	nanocubes	cubeoctahedrons	nanospheres
$E(3)$ [meV/bond]	277.8	287.3	0
$E(4)$ [meV/bond]	0	161.1	426.3
$E(5)$ [meV/bond]	217.9	243.4	258.3
$E(6)$ [meV/bond]	0	163.1	232.0
$E(7)$ [meV/bond]	0	239.5	212.2
$E(8)$ [meV/bond]	165.7	170.3	181.1
$E(9)$ [meV/bond]	0	162.2	159.2
$E(10)$ [meV/bond]	0	93.6	100.7
$E(11)$ [meV/bond]	0	16.9	46.0

TABLE II: Fitted coefficients $E(i)$, with i expressing the coordination of atoms (i.e., $12 - i$ is the number of bb), for the excess energy expression, Eq. 10.

(assuming $\sigma = \gamma$):

$$\frac{\mathcal{E}_\sigma}{\mathcal{E}_\gamma} = \frac{2(1 - 2\nu)}{E} \frac{\gamma}{R}. \quad (13)$$

Taking a representative values for gold, $\gamma = 1 \text{ J/m}^2$, $E = 78 \text{ GPa}$, and $R = 1 \text{ nm}$, Eq. 13 yields 0.359×10^{-2} , i.e. the surface stress contribution to the total excess energy is less than 1% of the surface induced excess energy. This ratio becomes even smaller (negligible) for larger nanospheres.

To corroborate this rather simplistic estimation, we plot in Fig. 7 the excess energy distribution over a cross section including the centre of a nanosphere (Fig. 7a) and nanocube (Fig. 7b) as obtained from the MD simulations. Several observations can be made. Firstly, the excess energy is concentrated at the nanoparticle surface irrespective of its shape. Since the surface stresses (and hence the volume strain energy) should be only important in the case of nanosphere, we can conclude that this contribution is effectively zero (or negligible), as the spacial distribution is very similar to the case of nanocube. Secondly, the excess energy is concentrated at the nanocube edges (corner of the cross section in Fig. 7b). This nicely agrees with the fitted values of $E_{\text{edge}} = 217.9 \text{ meV/bond}$ being larger than $E_{\text{facet}} = 165.7 \text{ meV/bond}$, estimated in section III C.

We therefore conclude, that even though the term surface energy was used in a slightly sluggish way throughout the section III B (more accurate would be to talk about surface induced excess energy), the energy contribution of surface stresses can be neglected and the two quantities, surface energy and surface induced excess energy, are for practical cases with nanoparticles larger than $\approx 1 \text{ nm}$ equivalent.

IV. CONCLUSIONS

A molecular dynamics study, complemented by first principles Density Functional Theory calculations, was performed to address surface energy of small gold nanoclusters of various sizes and (geometrically well defined) shapes. The employed interatomic pair potential was shown to give structural parameters and surface energies comparable with DFT-LDA calculations. The surface energy of nanocubes and nanospheres was shown to converge to a constant value. The convergence was faster in the case of nanospheres, where γ is practically constant for any particles with radius larger than $\approx 3 \text{ nm}$. Truncated cubes (cubeoctahedrons) did not achieve a single value for the surface energy within the studied range of nanoparticle sizes, but instead oscillated between two values. The range of these oscillations equals to the difference between γ of (100) and (111) facets. Finally, the surface-induced excess energy is suggested to follow a universal power-law dependence on the number of atoms forming the nanoparticle and is, to a large extent, related to a number of broken bonds (reduced coordination of the surface atoms). This explains the trend of decreasing surface energy with increasing nanoparticle size.

As other theoretical studies, also this study has found an increase of the surface energy with decreasing particle size. This should not be confused with experimental works on liquid–solid interface energies of gold nanoparticles, moreover often having irregular shapes. This work contributes to understanding of surface energy (solid phase–vacuum interface) and its relation to the nanoparticle structure.

* david.holec@unileoben.ac.at

¹ Y. Chen, X. Gu, C.-G. Nie, Z.-Y. Jiang, Z.-X. Xie, and C.-J. Lin, Chem. Commun., 4181 (2005).

² M. Grzelczak, J. Pérez-Juste, P. Mulvaney, and L. M.

Liz-Marzán, Chem. Soc. Rev. **37**, 1783 (2008).

³ D. Vollath and F. D. Fischer, in *Metal Nanopowders: Production, Characterization, and Energetic Applications*, edited by A. A. Gromov and U. Teipel (Wiley, 2014) pp.

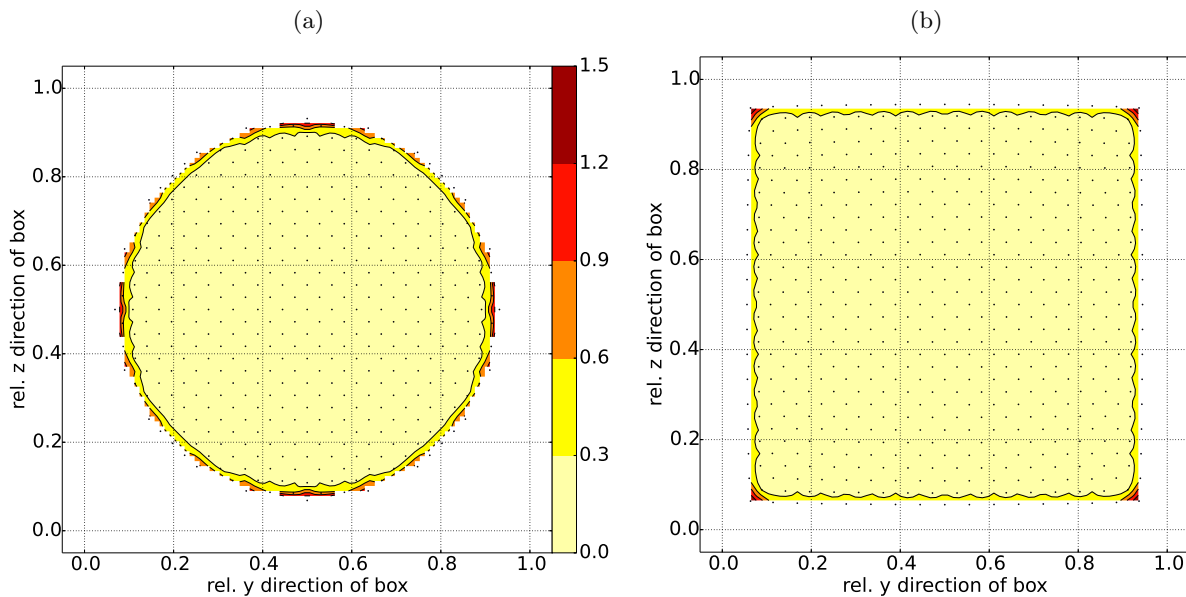


FIG. 7: Contour plots of the surface induced excess energy (per atom) distribution for cross sections of (a) nanosphere ($R = 3.25$ nm) and (b) nanocube ($a = 6.92$ nm). Both cross sections include the nanoparticle centre. The dots represent actual atoms in the cross section, e.g. real locations where the excess energy is stored. For the sake of clear demonstration, the discrete data were interpolated over the whole cross sectional area.

1–24.

⁴ A. Safaei and M. Attarian Shandiz, *Phys. Chem. Chem. Phys.* **12**, 15372 (2010).

⁵ M. Attarian Shandiz and A. Safaei, *Mater. Lett.* **62**, 3954 (2008).

⁶ J. Chang and E. Johnson, *Philos. Mag.* **85**, 3617 (2005).

⁷ B. Medasani, Y. H. Park, and I. Vasiliev, *Phys. Rev. B Condens. Matter* **75**, 235436 (2007).

⁸ B. Medasani and I. Vasiliev, *Surf. Sci.* **603**, 2042 (2009).

⁹ K. K. Nanda, A. Maisels, and F. E. Kruijs, *J. Phys. Chem. C* **112**, 13488 (2008), <http://dx.doi.org/10.1021/jp803934n>.

¹⁰ K. K. Nanda, A. Maisels, F. E. Kruijs, H. Fissan, and S. Stappert, *Phys. Rev. Lett.* **91**, 106102 (2003).

¹¹ S. Plimpton, *J. Comput. Phys.* **117**, 1 (1995).

¹² G. Grochola, S. P. Russo, and I. K. Snook, *J. Chem. Phys.* **123**, 204719 (2005).

¹³ F. Birch, *Physical Review* **71**, 809 (1947).

¹⁴ G. Kresse and J. Furthmüller, *Phys. Rev. B* **54**, 11169 (1996).

¹⁵ G. Kresse and J. Furthmüller, *Comput. Mater. Sci.* **6**, 15 (1996).

¹⁶ P. Hohenberg and W. Kohn, *Physical Review* **136**, B864 (1964).

¹⁷ W. Kohn and L. J. Sham,

Physical Review **140**, A1133 (1965).

¹⁸ Y. Wang and J. P. Perdew, *Phys. Rev. B* **44**, 13298 (1991).

¹⁹ G. Kresse and D. Joubert, *Phys. Rev. B* **59**, 1758 (1999).

²⁰ D. Holec and P. H. Mayrhofer, *Scripta Mater.* **67**, 760 (2012).

²¹ L. Vitos, A. V. Ruban, H. L. Skriver, and J. Kollár, *Surf. Sci.* **411**, 186 (1998).

²² E. Kozeschnik, I. Holzer, and B. Sonderegger, *J. Phase Equilib. Diffus.* **28**, 64 (2007).

²³ P. Haas, F. Tran, and P. Blaha, *Phys. Rev. B* **79**, 085104 (2009).

²⁴ v. Crljen, P. Lazić, D. Šokčević, and R. Brako, *Phys. Rev. B* **68**, 1 (2003).

²⁵ I. Galanakis, N. Papanikolaou, and P. H. PH, *Surf. Sci.* **511**, 1 (2002).

²⁶ W. Tyson and W. Miller, *Surf. Sci.* **62**, 267 (1977).

²⁷ D. Holec, M. A. Hartmann, F. D. Fischer, F. G. Rammerstorfer, P. H. Mayrhofer, and O. Paris, *Phys. Rev. B* **81**, 235403 (2010).

²⁸ N. Mameka, J. Markmann, H.-J. Jin, and J. Weissmüller, *Acta Mater.* **76**, 272 (2014).

²⁹ P. Müller, A. Saül, and F. Leroy, *Advances in Natural Sciences: Nanoscience and Nanotechnology* **5**, 01 (2008).

³⁰ F. D. Fischer, T. Waitz, D. Vollath, and N. K. Simha, *Prog. Mater. Sci.* **53**, 481 (2008).